ANNUAL REVIEWS

Double and Charge-Transfer Excitations in Time-Dependent Density Functional Theory

Neepa T. Maitra

Department of Physics, Rutgers University at Newark, Newark, New Jersey, USA;
email: neepa.maitra@rutgers.edu

Keywords

time-dependent density functional theory, TDDFT, excitations, adiabatic approximation

Abstract

Time-dependent density functional theory has emerged as a method of choice for calculations of spectra and response properties in physics, chemistry, and biology, with its system-size scaling enabling computations on systems much larger than otherwise possible. While increasingly complex and interesting systems have been successfully tackled with relatively simple functional approximations, there has also been increasing awareness that these functionals tend to fail for certain classes of approximations. Here I review the fundamental challenges the approximate functionals have in describing double excitations and charge-transfer excitations, which are two of the most common impediments for the theory to be applied in a black-box way. At the same time, I describe the progress made in recent decades in developing functional approximations that give useful predictions for these excitations.

1. INTRODUCTION

The response properties of an atom, molecule, or solid are a crucial aspect of its characterization. In poking a system with a perturbation, be it sunlight, a weak laser, or a collision with a small particle, one causes a gentle disturbance in its constituents whose consequent dynamics reveals a wealth of information about interactions in the system. Depending on how the timescales involved in the perturbation compare to the effective reaction times of the constituents, different types of correlation can be revealed: Sometimes only the electronic system is probed, while other times it is the vibrational or rotational motion of the ions that responds, or a combination of these. When the perturbation is weak enough that the system response scales linearly with the strength of the perturbation, the response at different frequencies and different wave vectors, i.e., the absorption spectrum, shows peaks at excitation energies of the system whose strength indicates the transition probability from the ground to that excited state.

Thus, the spectrum, meaning the excitation energies as well as their oscillator strengths, provides a unique signature of the system. Theoretical computations attempt to forge these signatures to make predictions of dynamics and processes, to identify or characterize an experimental spectrum, and to design new materials with some desired spectral property. Solving Schrödinger's equation for the many-electron system, however, scales exponentially with the number of electrons, so some kind of approximation is ultimately called for. Time-dependent density functional theory (TDDFT) provides a route to computing the absorption spectra that has achieved the best overall balance between accuracy and efficiency. Formulated in 1984 (1), with the linear-response framework developed in 1995 (2, 3), the past 25 years have seen some very exciting applications for response properties. The functional approximations that were used in the early days of TDDFT are often still used today. However, there are certain excitations for which these approximations perform poorly, and more sophisticated approximations are needed. Perhaps the most important cases of this are double excitations and charge-transfer excitations.

Both double and charge-transfer excitations are not merely of theoretical interest but also have important practical importance in a number of situations, from photovoltaic design to organic molecules to biochemical processes. This is particularly true when there is coupling to ionic motion and the molecule explores a wide range of geometries. There has therefore been a tremendous effort to describe these excitations not just within TDDFT but also with other many-body wave-function methods. I note that these excitations can also be challenging for wave-function methods: For example, the error in equation-of-motion coupled-cluster methods is related to the amount of double excitation in the transition (4). The general problem of computing accurate excited states has inspired the development of the QuestDB database, which has more than 500 highly accurate vertical excitations of different natures (5) in small- and medium-sized molecules, using only computational data.

This review focuses on the TDDFT description of these two classes of excitations. I begin with a review of how linear-response calculations proceed in TDDFT (Section 2) before first addressing the challenge, and some solutions, in obtaining double excitations in Section 3, and charge-transfer excitations in Section 4. I provide an outlook in Section 5.

2. TDDFT LINEAR RESPONSE

In a nutshell, TDDFT is an exact reformulation of the quantum dynamics of many-body systems, in which a noninteracting system of N electrons reproduces the one-body density of the true system (1, 6–9), $n(\mathbf{r}, t) = N \sum_{\sigma, \sigma_2 \ldots \sigma_N} \int |\Psi(\mathbf{r}\sigma, \mathbf{r}_2\sigma_2 \ldots \mathbf{r}_N\sigma_N)|^2 d^3r_2 \ldots d^3r_N$. Instead of finding the true correlated wave function, a problem that scales exponentially with the number of

electrons, one need only find a set of N orbitals that satisfies the time-dependent Kohn-Sham (KS) equations

$$\left[-\frac{\hbar^2}{2m}\nabla^2 + v_S(\mathbf{r},t) \right]\phi_k(\mathbf{r},t) = i\partial_t\phi_k(\mathbf{r},t),\qquad 1.$$

where the KS potential $v_S(\mathbf{r},t) = v_{\text{ext}}(\mathbf{r},t) + v_H[n](\mathbf{r},t) + v_{\text{XC}}[n;\Psi_0,\Phi_0](\mathbf{r},t)$ with the Hartree potential $v_H[n](\mathbf{r},t) = \int \frac{n(\mathbf{r}',t)}{|\mathbf{r}-\mathbf{r}'|}d^3r'$ is the classical electrostatic repulsion of the electron distribution, and $v_{\text{XC}}[n;\Psi_0,\Phi_0](\mathbf{r},t)$ is the exchange-correlation (xc) potential that is defined such that the time-evolving density of the occupied orbitals is identical to the true density, $n(\mathbf{r},t) = \sum_{k,\text{occ}}|\phi_k(\mathbf{r},t)|^2$. Atomic units where $e^2 = \hbar = m_e = 1$ are used throughout this article unless otherwise stated. The xc potential is a functional of the density, including its history, as well as the initial interacting state Ψ_0 and noninteracting state Φ_0; when the dynamics begins in the ground state, as in the linear-response regime, the initial-state dependence is usurped into the density dependence by the Hohenberg-Kohn theorem of ground-state DFT (10), and the xc potential may be simply written as $v_{\text{XC}}[n](\mathbf{r},t)$.

In practice, of course, v_{XC} is unknown and approximations are made, most of which simply insert the instantaneous density into a ground-state approximation. This adiabatic approximation thus completely neglects both the history and initial-state dependence, yet has led to many useful predictions in both the linear response as well as the nonperturbative regime (see Reference 8, and references therein). In the past couple of decades, there has been an increased understanding of where and why the functional approximations fail, especially in the linear-response regime, such that users know when to trust their TDDFT results using standard functionals and when to be cautious. More sophisticated functionals have been developed from first principles, which, while computationally more involved, deliver more reliable results for classes of excitations for which the standard approximations fail. Two of these classes, double and long-range charge-transfer excitations, are the focus of this review.

When applied to linear response, the formalism and its functionals simplify. First-order perturbation theory gives the linear response of the density to a perturbation $\delta v(\mathbf{r},t)$

$$n^{(1)}(\mathbf{r},t) = \int_0^\infty dt' \int d^3r'\,\chi(\mathbf{r}t,\mathbf{r}'t')\delta v(\mathbf{r}'t'),\qquad 2.$$

where in the frequency domain the density–density response function χ has poles at the exact frequencies $\Omega_j = E_j - E_0$. In addition, the residues give transition densities between the true ground Ψ_0 and excited Ψ_j many-body states

$$\chi(\mathbf{r},\mathbf{r}',\omega) = \sum_j \frac{\langle\Psi_0|\hat{n}(\mathbf{r})|\Psi_j\rangle\langle\Psi_j|\hat{n}(\mathbf{r}')|\Psi_0\rangle}{\omega - \Omega_j + i0^+} + c.c.(-\omega),\qquad 3.$$

where $\hat{n}(\mathbf{r}) = \sum_i \delta(\mathbf{r}-\mathbf{r}_i)$ is the one-body density operator. The notation $c.c.(-\omega)$ denotes the complex conjugate of the first term at frequency $-\omega$. Equation 3 involves a sum over excited states; the $j = 0$ terms in the first and second terms cancel. Using the fact that the time-dependent KS system yields the same density as the interacting system, TDDFT provides an expression for the response function χ that bypasses finding the excited states (3, 11),

$$\chi[n](\mathbf{r},\mathbf{r}',\omega) = \chi_S[n](\mathbf{r},\mathbf{r}',\omega) + \int d^3r_1 d^3r_2\,\chi_S(\mathbf{r},\mathbf{r}_1,\omega)\left[\frac{1}{|\mathbf{r}_1-\mathbf{r}_2|} + f_{\text{XC}}(\mathbf{r}_1,\mathbf{r}_2,\omega) \right]\chi(\mathbf{r}_2,\mathbf{r}',\omega),\quad 4.$$

where

$$\chi_S[n](\mathbf{r},\mathbf{r}',\omega) = \lim_{\eta\to 0^+}\sum_{k,j}(f_k - f_j)\delta_{\sigma_k,\sigma_j}\frac{\phi_k^*(\mathbf{r})\phi_j(\mathbf{r})\phi_j^*(\mathbf{r}')\phi_k(\mathbf{r}')}{\omega - (\epsilon_j - \epsilon_k) + i\eta}\qquad 5.$$

is the time-frequency Fourier transform of $\chi_S(\mathbf{r}, \mathbf{r}', t - t') = \frac{\delta n(\mathbf{r},t)}{\delta v_S(\mathbf{r}',t')}$, and the xc kernel is that of $f_{XC}[n](\mathbf{r}, \mathbf{r}', t - t') = \frac{\delta v_{XC}[n](\mathbf{r},t)}{\delta n(\mathbf{r}'t')}$. In Equation 5, f_i are Fermi occupation numbers of the orbital i in the ground-state KS determinant and σ_i indicates the spin of the orbital i.

Equation 4 is the central equation in TDDFT linear response (3), showing how the excitation energies and transition densities of the true interacting system are related to those of the non-interacting KS system and the xc kernel. In practice, although this is used directly for extended systems, for molecules a matrix formulation is used (2, 11). There are several versions that are all essentially equivalent (6, 12, 13) and involve solving for eigenvalues and eigenvectors of a matrix in the basis of KS single excitations. In the Casida formulation (2, 11, 13), we have

$$R(\Omega_j)F_j = \Omega_j^2 F_j \qquad 6.$$

(provided the orbitals are chosen real), where

$$R_{qq'}(\omega) = \omega_q^2 \delta_{qq'} + 4\sqrt{\omega_q \omega_{q'}} \int d^3 r d^3 r' \Phi_q(\mathbf{r}) \left[\frac{1}{|\mathbf{r} - \mathbf{r}'|} + f_{XC}(\mathbf{r}, \mathbf{r}', \omega) \right] \Phi_{q'}(\mathbf{r}'), \qquad 7.$$

with $q = i \to a$ denoting a single KS excitation from an occupied orbital i to unoccupied a, and $\Phi_q(\mathbf{r}) = \phi_i^*(\mathbf{r})\phi_a(\mathbf{r})$ a KS transition density. In Equation 7, we have restricted ourselves to spin-saturated, closed-shell systems for simplicity; the spin-dependent versions of these equations yield singlet-triplet splittings. The eigenvalues of R yield the excitation energies Ω_j, while the true transition densities and oscillators are related to the eigenvectors f_j.

Two truncations of Equation 4 or Equation 7 are particularly useful tools for analysis. In the small matrix approximation (SMA), we focus on one KS excitation and assume it has negligible coupling to the other excitations. Then (3, 12–14),

$$\Omega^{SMA} = \sqrt{\omega_q^2 + 4\omega_q \int d^3 r d^3 r' \Phi_q(\mathbf{r}) f_{HXC}(\mathbf{r}, \mathbf{r}', \omega) \Phi_q(\mathbf{r}')}, \qquad 8.$$

where the notation HXC denotes Hartree-xc, $f_{HXC} = \frac{1}{|\mathbf{r}-\mathbf{r}'|} + f_{XC}$. If, additionally, the correction to the KS excitation frequency ω_q is itself much smaller than ω_q, taking a Taylor expansion yields the single pole approximation (SPA)

$$\Omega^{SPA} = \omega_q + 2 \int d^3 r d^3 r' \Phi_q(\mathbf{r}) f_{HXC}(\mathbf{r}, \mathbf{r}', \omega) \Phi_q(\mathbf{r}'). \qquad 9.$$

In principle, use of the exact ground-state xc potential and exact xc kernel in Equation 4 or Equation 7 would yield exact excitation energies and transition densities of the physical system. However, both of these ingredients are unknown and need to be approximated in practice. The choices for the ground-state functional are enormous (15–18) and vary hugely in their degree of empiricism as well as in their computational cost. For the xc kernel, the adiabatic approximation for the xc potential translates to a frequency-independent f_{XC}, which follows from $v_{XC}^A[n](\mathbf{r}, t) = v_{XC}^{g.s.}[n(t)](\mathbf{r})$, then $f_{XC}[n](\mathbf{r}, \mathbf{r}', t - t') = \frac{\delta^2 E_{XC}[n]}{\delta n(\mathbf{r})\delta n(\mathbf{r}')}\delta(t - t')$, so

$$f_{XC}^A[n](\mathbf{r}, \mathbf{r}', \omega) = \left. \frac{\delta^2 E_{XC}[n]}{\delta n(\mathbf{r})\delta n(\mathbf{r}')} \right|_{n=n(\mathbf{r})}. \qquad 10.$$

In the following sections, we analyze what the challenges are in using linear-response TDDFT for double excitations and charge-transfer excitations, as well as possible solutions, from the perspectives of both Equations 4 and 7. Both expressions demonstrate the key role played by the xc kernel in producing the response of the interacting system from that of the KS one, but also the key role played by the bare KS excitations themselves as a zeroth order starting point for the

TDDFT machinery. We will see that, while the structure of the kernel is the crucial aspect in capturing double excitations and charge-transfer excitations between open-shell fragments, a good approximation for the ground-state potential is a crucial aspect of getting charge transfer between closed-shell fragments correct.

Before doing so, we note that there are two other formulations of linear response within TDDFT that may be more computationally efficient for certain situations. The Sternheimer approach, also known as density perturbation theory or coupled perturbed KS, avoids the calculation of unoccupied states by instead considering perturbations of the occupied KS orbitals in the frequency domain (19, 20). Also avoiding unoccupied orbitals, one can Fourier transform the real-time propagation of occupied orbitals under a weak perturbation, often using a δ-kick in time to uniformly stimulate the entire spectrum (21).
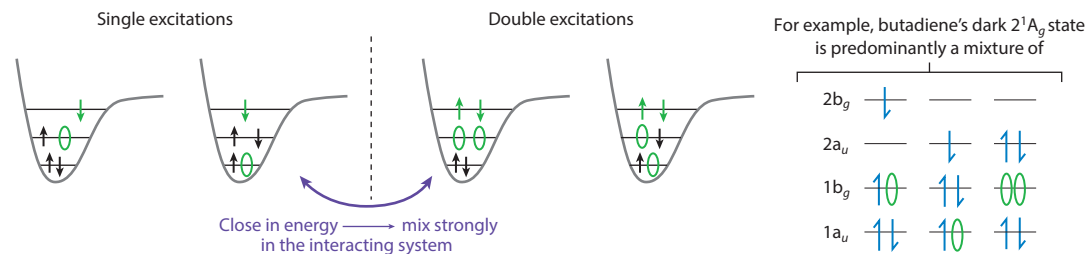
3. DOUBLE EXCITATIONS

First, what is a double excitation? The term is a shorthand for a state of double-excitation character and has meaning in the context of noninteracting reference systems such as Hartree-Fock or KS DFT (22). In these systems, one has N orbitals that are occupied in the ground state, where N is the number of electrons, and an infinite number of virtual orbitals. A doubly excited Slater determinant is when two electrons are promoted out of occupied orbitals into two virtual orbitals, and a double excitation of the true interacting system is then one that has a significant proportion of doubly excited determinants in an expansion of the true correlated state, using the noninteracting reference states (see also **Figure 1**). Clearly, the details of the expansion coefficients and the orbitals themselves are dependent on which noninteracting reference is chosen. Whether a given state should be classified as a single excitation (usually meaning a linear combination of single excitations, again with respect to a chosen noninteracting reference) or a double or multiple excitation, generally then depends on the choice of the reference. Note, though, that for a given reference, a well-defined and unambiguous classification can be made by following the states as the interaction is slowly turned down to zero. For DFT references, this is done along the adiabatic connection curve, and the procedure is described in Reference 23 (see also discussion in Reference 24).

But this definition relying on the notion of a noninteracting reference means that whether a state is classified as being a double excitation or not can lose intrinsic meaning. A double excitation using a single determinant reference, such as Hartree-Fock or KS DFT, may appear as single excitations from a multireference ground state or if excited-state orbital-relaxation is accounted for, such as has been discussed for the case of butadiene, for example (4, 25, 26). However, within TDDFT no such ambiguity arises, because the KS ground state is a Slater determinant (except in cases of strict degeneracy), and the excitations are obtained within a fixed basis of occupied and unoccupied orbitals once the ground state is determined; i.e., there is no orbital relaxation as such. Thus, the double-excitation character of the state is well-defined in TDDFT, determined by the path of Reference 23.

Now we turn to how double excitations appear in the linear response spectrum. In fact, they are completely absent in the KS linear response, and it is purely through their interaction with a single excitation that they appear in the true response function, as we now will demonstrate. We consider expanding the true interacting states $|\Psi_j\rangle$ in the complete set formed by KS determinants

$$|\Psi_j\rangle = C_0^j|\Phi_0\rangle + \sum_q C_q^j|\Phi_q\rangle + \sum_D C_D^j|\Phi_D\rangle + \dots, \qquad 11.$$

a Single versus double excitations

Single excitations

Double excitations

For example, butadiene's dark 2^1A_g state is predominantly a mixture of

2b_g
2a_u
1b_g
1a_u

Close in energy ——→ mix strongly in the interacting system

b Auto-ionizing resonances and Auger processes

Bound double excitation with energy in the continuum

Single excitation to the continuum

a
i

$\omega = 2(\varepsilon_a - \varepsilon_i)$

ω

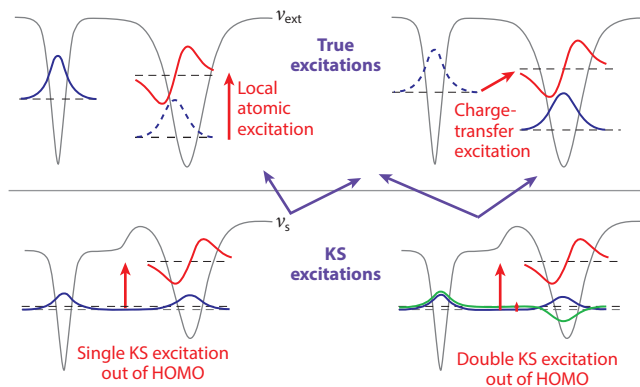Mix strongly in the interacting system ——→ Fano resonance

For example, lowest double excitation in helium ($2s^2$)
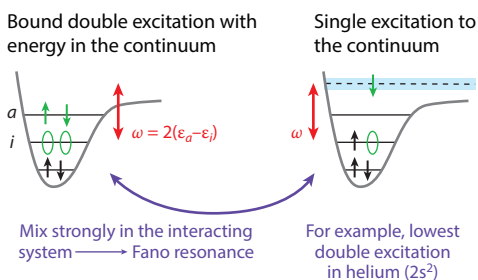
c Excitations of molecule of open-shell moieties

v_{ext}

True excitations

Local atomic excitation

Charge-transfer excitation

v_s

KS excitations

Single KS excitation out of HOMO

Double KS excitation out of HOMO

Figure 1

Double excitations in different contexts. (*a*) Single versus double excitations, defined with respect to a single-determinant reference such as KS, and the example of the butadiene 2^1A_g state, which is a mixture of two single and one double excitations out of the KS single Slater determinant reference. (*b*) Auto-ionizing resonances often involve double excitations in which, in a single-particle reference, a double excitation to a bound orbital has an energy that lies in the continuum. Once electron interaction is accounted for, the state turns into a resonance, and TDDFT with a frequency-dependent kernel can give approximate line widths (22). (*c*) Excitations of a stretched molecule exemplify the ubiquity of double excitations when static correlation is present. Abbreviations: HOMO, highest occupied molecular orbital; KS, Kohn-Sham; TDDFT, time-dependent density functional theory.

where $q = i \rightarrow a$ represents all single excitations out of the KS ground-state determinant Φ_0, and $D = (i \rightarrow a, j \rightarrow b)$ represents all double excitations, etc. The numerator of Equation 3 involves matrix elements between the ground and excited states of the density-operator $\hat{n}(\mathbf{r})$, which, being a one-body operator, has only nonzero elements between determinants that differ by at most one orbital. For this reason, even before considering χ, it is instructive to apply Equation 3 to the noninteracting KS system, where the numerator involves $\langle \Phi_j | \hat{n}(\mathbf{r}) | \Phi_0 \rangle$: Only the single excitations $\langle \Phi_j | = \langle \Phi_q |$ give a nonzero contribution. Physically, this is to be expected, because a double excitation in a noninteracting system would mean that two electrons are excited, a process that would require two photons, and so would scale quadratically in the perturbation strength, not linearly.

Returning to the interacting system, it follows from above that if the true ground state is weakly correlated and well-approximated by a Slater determinant, then excited states of double-excitation character $|\Psi_j\rangle$ contribute to the linear response solely through their single-excitation component $|\Phi_q\rangle$ in the expansion of Equation 11. More generally, putting the expansion of Equation 11 for $|\Psi_0\rangle$ and $|\Psi_j\rangle$ into Equation 3, we see that the $|\Phi_0\rangle$ component of the interacting ground state $|\Psi_0\rangle$ gives a nonzero contribution only through matrix elements with the single-excitation components

$|\Phi_q\rangle$ of the excited state $|\Psi_j\rangle$, while the single-excitation components of the ground state ($|\Phi_q\rangle$ in the expansion of $|\Psi_0\rangle$) give a nonzero contribution through the double-excitation component $|\Phi_D\rangle$ of the excited state, and the double-excitation component of the ground state connects to the single excitation and any triple-excitation components of the excited state. Likewise, the double-excitation component of the excited state connects only to the single excitation and any triple-excitation components of the ground state. As triple excitations are generally much higher in energy, we see that the double excitations really contribute only through couplings with the single excitations. There are clearly more poles in the interacting χ than in the KS χ_S: χ has poles at true states that are linear combinations of single, double, and higher excitations, while χ_S has poles only at single excitations.

Given that in TDDFT χ is obtained from χ_S through Equation 4, the appearance of double excitations in χ depends entirely on the xc kernel. That is, unlike single excitations, there is no zeroth order approximation to the double excitation that can be extracted from the response function or in Casida's matrix. One could resort to taking sums of the KS single excitations as a zeroth order approximation, but such a term does not naturally arise in the TDDFT linear-response formalism. Further, to generate more poles than the KS system has, the xc kernel must be strongly frequency dependent. Another way to see this is through the matrix equation, Equation 7. As this is a matrix that spans only single excitations, the only way that information about a double excitation can enter is implicitly through f_{XC}. Because the interacting system has a larger number of excitations than do the noninteracting ones, the equation must represent a nonlinear rather than a linear eigenvalue problem, which arises due to the frequency dependence of the xc kernel (22, 27–30).

The lack of double excitations in the adiabatic approximation was noted soon after TDDFT linear response was formulated (27, 28), when it was also suspected that including frequency dependence would unveil them. Reference 31 numerically demonstrated the need for frequency dependence to capture double excitations by showing that the adiabatically exact approximation misses their peaks in the absorption spectrum. The adiabatically exact approximation is the best that an adiabatic approximation could hope to be, as it inputs the instantaneous density into the exact ground-state xc functional. This can be done only for model systems in which the exact ground-state xc functional is numerically accessible; to demonstrate this, Thiele & Kümmel (31) ran real-time propagation on some one-dimensional, two-electron systems in the linear-response regime.

An explicit computation of the frequency dependence of the exact xc kernel is quite a computational feat, given that it is effectively solving an inverse problem that is very sensitive to small errors. Yet it has been achieved (32–34) on model systems, and results verify the simple pole structure of the xc kernel near double or multiple excitations that was postulated in a simple model in Reference 29 (Section 3.1). Thiele & Kümmel (32) performed real-time calculations of a kick perturbation that is localized in space and time to effectively find the functional derivatives in $\chi(\mathbf{r}, \mathbf{r}', t - t')$ and $\chi_S(\mathbf{r}, \mathbf{r}', t - t')$, then Fourier transformed them to the frequency domain to reveal a full spatial and frequency dependency of the kernel, $f_{XC} = \chi_S^{-1} - \chi^{-1} - 1/|\mathbf{r} - \mathbf{r}'|$. Entwistle & Godby (33) and Woods et al. (34) worked directly in the frequency domain to construct the true and KS response functions. In both approaches, regions of small density need extra attention; a thorough analysis together with different ways to deal with this can be found in Reference 34. An interesting issue that arose is the gauge freedom of the xc kernel (34–36): Adding functions $g(\mathbf{r}, \omega)$ (independent of $\mathbf{r}'$), $h(\mathbf{r}', \omega)$ (independent of $\mathbf{r}$), or a spatially independent term to $f_{XC}(\mathbf{r}, \mathbf{r}', \omega)$ has no effect in the Dyson equation (Equation 4). This reflects the fact that the physics is invariant under a spatially uniform but possibly time-dependent shift of the potential. These studies used the soft-Coulomb interaction between electrons that is often used in one-dimensional models. An exact analytic expression for the xc kernel has also been shown on two different models with

different interactions: one for a ring geometry with a squared cosine interaction (37), and the other for a lattice system, the (a)symmetric Hubbard dimer (38–41).

3.1. Dressed TDDFT

To reveal the hidden double excitations in f_{XC}, Maitra, Zhang, Cave, and Burke (29) considered a simple idealized situation in which, in the KS system, one double excitation is close in energy to a single excitation, and both are far away from all other excitations, such that in the frequency range near these two states, the KS response function has a single pole. Electron interaction mixes these two excitations such that there are two excitations in the interacting system that are linear combinations of this KS single and double, each contributing a distinct pole in the response function χ. Motivated by the expression obtained from solving Equation 7 in this subspace for f_{XC}, we (29) asserted the dressed SPA (dSPA) for the xc kernel

$$\int d^3r d^3r' \Phi_q(\mathbf{r}) f_{XC}^{dSPA}(\mathbf{r}, \mathbf{r}', \omega) \Phi_q(\mathbf{r}') = \int d^3r d^3r' \Phi_q(\mathbf{r}) f_{XC}^{A}(\mathbf{r}, \mathbf{r}') \Phi_q(\mathbf{r}') + \frac{|H_{qD}|^2/2}{\omega - (H_{DD} - H_{00})}, \quad 12.$$

where the second term gives a frequency-dependent correction to a chosen adiabatic approximation (first term) involving Hamiltonian matrix elements with the KS single (q), double (D), and ground state (0). (A sketch is shown in **Figure 2**.) The kernel was proposed as an a posteriori correction to the adiabatic approximation, which was applied to just the particular KS single excitation that lies near a double excitation. Its derivation relies on the idea that the interactions of these two excitations with the other KS excitations in the system are far weaker than those with each other. If several KS single excitations mix significantly with a double excitation, then the dressing can be applied in a matrix spanned by those singles, in a dressed Tamm-Dancoff scheme, as was done for small polyenes in References 42–44 (see also **Figure 1a**). Gritsenko & Baerends (45) unveiled the spatial dependence of the kernel and, using the common energy denominator approximation, could approximately account for the effect of the entire spectrum on the coupled singly and doubly excited states.

Several related and more rigorously based approaches have led to kernels of essentially the same form as Equation 12. Casida (46) used the equation-of-motion superoperator approach to derive a polarization propagator equation, separating out the adiabatic and nonadiabatic contributions. The nonadiabatic part was shown to reduce to Equation 12 in the special case in
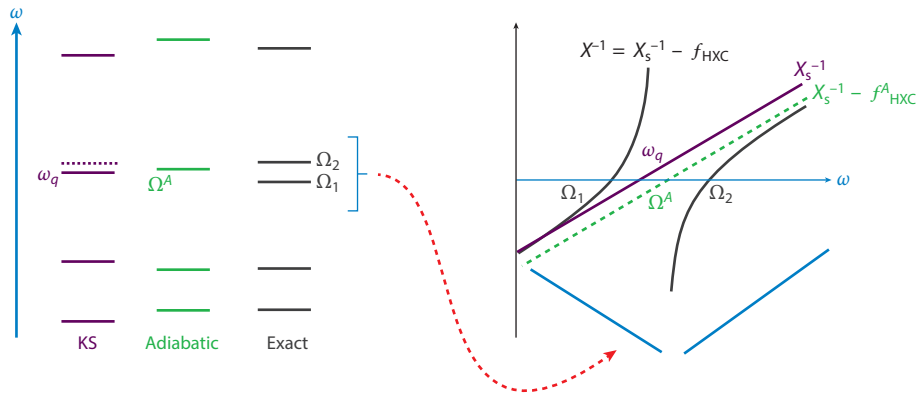
Figure 2

Schematic illustration showing how the frequency dependence in the dressed kernel generates an extra pole. Abbreviations: HXC, Hartree exchange correlation; KS, Kohn-Sham.

which the ground state is closed-shell, while in the general case, it provides an extension of dressed TDDFT to open-shell doublets. Romaniello et al. (47) built an xc kernel from contracting the four-point Bethe-Salpeter equation of many-body theory to the two-point one of TDDFT (48, 49). Usually a static approximation is used for the many-body kernel, but Romaniello et al. (47) showed that a frequency-dependent screened Coulomb interaction is crucial to capturing these states; the frequency dependence of the TDDFT xc kernel extracted from this has two origins, one from the folding of the space variables, and the other from this explicit dependence. This approach, however, led to spurious excitations that were thought to be due to a self-screening error and later were shown to be avoidable by imposing a condition for number conservation in the Bethe-Salpeter approach (50). The relation between this approach and the propagator approach was clarified in Reference 51.

The dressed kernel has been tested on a range of different molecules, computing excited state geometries as well as energies (43, 44, 52). An extensive study using the development version of the deMon2k code (53) on 28 organic molecules suggested that dressed TDDFT gives the best results when the adiabatic kernel it is paired with is a hybrid.

Still, there are double excitations for which the dressed kernel does not apply, namely when the condition that the subspace containing the double excitation be uncoupled from the others, in particular the ground state, does not hold. When the KS lowest unoccupied molecular orbital (LUMO) energy lies low close to a doubly occupied highest occupied molecular orbital (HOMO) energy, any single excitation out of the HOMO will be near degenerate, with a double excitation in which the other electron occupying the HOMO hops into the low-lying LUMO (54) (see also **Figure 1c**). This means that $f_{\mathrm{HXC}}(\omega)$ has a strong frequency dependence throughout the spectrum. It also means that the dressed kernel is not appropriate, as the SPA under which it is to be applied breaks down (12, 13, 55). Two relevant situations in which this occurs are conical intersections with the ground state (56) and stretched single bonds such as in dissociating diatomic molecules (54, 55, 57) (see Section 4.2). In these cases, ground-state DFT also struggles tremendously, because the single Slater determinant character of the KS state is so far from the exact ground state, which is strongly correlated.

While the frequencies give the position of the peaks in the absorption spectrum, an aspect of the spectrum that tends to be less discussed is the height of the peaks in the spectrum, that is, the oscillator strength. TDDFT gives, in principle, the exact oscillator strengths, which are extracted from the residues of the susceptibility χ or the eigenvectors of the matrix R of Equation 7 (2, 11–13); a recent benchmarking for general excitations in small compounds can be found in Reference 58. Casida (2) showed that frequency dependence of the xc kernel imposes a renormalization of the eigenvectors F_j of R compared to those obtained from the adiabatic approximation when computing the oscillator strengths (equations 4.39– 4.41 in Reference 2). To my knowledge, the effect this renormalization has on shattering the single KS peak strength into the mixed single- and double-character components has not been explored very much; I know of only one work on an asymmetric Hubbard dimer, discussed in Reference 41.

3.2. Searching for Doubles Elsewhere Within DFT

Although dressed TDDFT has successfully computed excitation energies of double excitations, it is not widely used; this is perhaps because it is not applied in a black-box way, as one first scans the single excitations out of an adiabatic approximation to see where to apply the frequency-dependent part of the kernel. I briefly mention here some other density-functional-based approaches that have been explored for double excitations.

A natural approach is to consider quadratic response: Given that two photons are required to excite two electrons in a noninteracting system, one might hope that an adiabatic approximation

used within quadratic response theory has the right structure to couple single and double KS excitations. Unfortunately, it was found (22, 59) that while adiabatic quadratic response does contain poles at the sum of linear-response-corrected KS single excitations, it misses the mixing between single KS excitations with these double excitations. Using the Tamm-Dancoff approximation in the linear-response part of the calculation makes even these poles disappear.

Back to linear response, instead of improving the xc kernel, spin-flip TDDFT instead modifies the reference state around which the linear response is performed (60, 61); this was originally introduced to access ground states of multireference character. A double excitation with respect to the ground state appears as a single excitation of the new reference state. Choosing a high-spin triplet state as reference and applying spin-flip excitations, double KS excitations contribute to the TDDFT linear response using the usual adiabatic xc kernels or noncollinear ones designed by considering the nature of the reference state (62).

An alternative linear-response theory was recently developed that is in a similar spirit to TDDFT but distinct in that the excitations involve electron additions or removals: In particle–particle random phase approximation (pp-RPA) (63, 64), the reference state is the ground state of $(N − 2)$ electrons instead of N. Then two electrons are added to any of the unoccupied orbitals of the reference; in this way, double excitations naturally arise. There are some limitations, depending on the character of the double excitation (e.g., it does not capture excitations in which a significant amount of the hole is in the HOMO-1), but it works well otherwise; it also works for other difficult excitations in TDDFT, including charge transfer.

Falling back to DFT, note that constrained variational methods have been formulated to reproduce excited states of a given character and have been applied to double excitations, in particular ΔSCF and orbital-optimized DFT (65), constricted variational DFT (66), and eXcited Constrained DFT (67).

Stepping outside standard KS DFT, a promising approach that has resurfaced in recent years is ensemble DFT (68–70). Ensemble DFT is based on the rigorous Gross-Oliveira-Kohn variational principle for ground and excited states, and its initial exposition predated the linear-response framework of TDDFT. Although early approximations for the functionals were not accurate enough to be useful (71, 72), very recent algorithmic and functional developments have reawakened the exploration of whether it could become a practical and accurate method, with computational cost similar to that of KS DFT. Several works have considered double excitations in this framework (73–76).

4. CHARGE-TRANSFER EXCITATIONS

A charge-transfer excitation is one in which a large fraction of the excited-state electron density is localized in a region with little spatial overlap with the density of the ground state. This occurs in a number of situations, for example, when the excited state is rotated with respect to the ground state, as in twisted intramolecular charge-transfer compounds, or at stretched geometries, as in a dissociating bond. In the limit of minimal overlap between the donor and acceptor states, one can obtain the lowest charge-transfer energy staying within a ground-state DFT by using constrained DFT (77). One can extract useful coupling matrix elements from the constrained states. For a general approach to charge transfer, one needs to consider TDDFT. Charge transfer plays a key role in many central processes in science, including photosynthesis, photovoltaic devices, molecular switches, nanoscale conductance, and reactions in solvents and at interfaces. In many of these applications, the systems are large enough that TDDFT is the only practical option, and so charge transfer has received a lot of attention. A detailed review of the issues and developments in both linear response and fully time-resolved, nonperturbative dynamics can be found in Reference 78.

In the early 2000s, it was realized that standard approximate TDDFT functionals severely underestimate charge-transfer excitation energies (79, 80). Yet, at around the same time, a TDDFT study made a breakthrough in the explanation of the charge-transfer process responsible for the dual fluorescence of 4-dimethyl-aminobenzonitrile (DMABN) in polar solvents, whose mechanism had until then remained a mystery (81). The nature of the red-shifted emission band had been thought to be due to an intramolecular charge-transfer state, but the lack of accurate but computationally efficient methods at the time made it difficult to know whether it had a twisted or planar quinoidal structure. Using TDDFT with the B3LYP functional, Rappoport & Furche (81) could without doubt identify the electronic and geometric nature of the state and the mechanism that led to the dual fluorescence. This was an early success story for TDDFT and charge-transfer processes, in which the underestimation of the charge-transfer excitation energies themselves was not important. They were indeed likely underestimated, but two aspects of the study meant that it did not affect the conclusions: First, the calculations were performed in the gas phase, while the phenomenon occurs in solvent that would tend to lower the excitation energy anyway, and second, the excited properties such as vibrational frequencies and force constants used to identify the state appear to be generally less sensitive. However, in general, the large underestimation of charge-transfer excitation energies hampers the predictivity of standard TDDFT approximations in a range of applications in physics, chemistry, and biology and has driven tremendous developments in the past decade or so, such that now first-principles nonempirical functional approximations are available that can in many cases yield reliable and predictive results for charge-transfer excitations (82).

For the ensuing discussion on why these excitations are so challenging for TDDFT, we need to first recall what their exact value should be. Consider an excitation of a stretched neutral molecule in which one electron has transferred from one end (the donor) to the other (the acceptor). Then, at large separations, the exact frequency of this excitation approaches

$$\Omega = I^D - A^A - 1/R, \qquad \qquad 13.$$

where $I^D = E^D(N_D - 1) - E^D(N_D)$ is the ionization energy of the N_D-electron donor, $A^A = E^A(N_A) - E^A(N_A + 1)$ is the electron affinity of the N_A-electron acceptor, and $-1/R$ is the electrostatic attraction between the fragments after the transfer, lowest order in the separation R.

How these excitations are represented in TDDFT depends on the character of the underlying KS orbitals. We must distinguish two cases: charge transfer between closed-shell fragments and between open-shell fragments. The latter case is particularly challenging for TDDFT because of the strongly correlated nature of the ground state, and the analysis of the situation is quite distinct from the former. Note that several diagnostics of the degree of charge transfer in an excitation have been useful (83–85).

4.1. Charge-Transfer Excitations Between Closed-Shell Fragments

In this case, we have a pair of electrons in the HOMO of the donor from which we transfer one to the LUMO of the acceptor. The Kohn-Sham orbital energy difference is then simply

$$\omega_q = \epsilon_L^A - \epsilon_H^D, \qquad \qquad 14.$$

and the TDDFT procedure of Equation 7 provides a diagonal correction and mixes this excitation with other excitations through the f_{XC}-matrix element that goes into $R_{qq'}$. However, it is evident from this equation that the KS transition density $\Phi_q(\mathbf{r}) = \phi_H^{D*}(\mathbf{r})\phi_L^A(\mathbf{r})$ is exponentially small as a function of the separation R, so for a nonvanishing correction to the KS orbital energy difference, $f_{XC}(\mathbf{r}, \mathbf{r}', \omega)$ must exponentially grow as a function of R. Local and semilocal functionals

[local density approximation (LDA)/generalized gradient approximation (GGA)] do not have this property, so their TDDFT excitation energy collapses to the orbital energy difference.

One might wonder, How far is the KS orbital energy difference $\omega_q = \epsilon_L^A - \epsilon_H^D$ from the exact charge transfer excitation energy (Equation 13)? The answer depends not only on what ground-state functional is being used but also on whether the calculation is performed within pure KS DFT or the generalized KS framework (86–88). There is a key difference between these two formalisms that has a significant consequence for charge-transfer excitations: in the former, unoccupied orbital energies are excitations of the neutral system, while in the latter, they have a character somewhere in between neutral and addition energies depending on the amount of Hartree-Fock that is mixed in. Given that charge-transfer excitations, albeit being overall neutral, do involve the addition of one electron on one moiety, the generalized KS may have a practical advantage. In the following, I briefly outline different approaches, considering the nature of the bare KS orbital energy differences as well as the TDDFT correction from f_{XC}, which for nonlocal functionals could be nonvanishing. I also consider several distinct and contrasting approaches, and again note that more detailed exposition is given in Reference 78.

First, if the exact ground-state functional is somehow known and used, then we have $\omega_q = I^D - A_S^A = I^D - A^A - \Delta_{XC}^A$, because in DFT the magnitude of the HOMO orbital energy is exactly equal to the true ionization energy, but the KS LUMO orbital energy differs from the electron affinity by the derivative discontinuity Δ_{XC}^A (78, 89–94). That is, the exact KS orbital energy difference is lacking relaxation contributions to the acceptor's electron affinity as well as the $-1/R$ behavior at large separations; if the exact ground-state functional was used in the TDDFT calculation, these terms would need to result from the f_{XC} term in Equation 7, and, from the discussion around Equation 13, one sees that this requires $f_{XC}(\mathbf{r}, \mathbf{r}', \omega)$ to have some matrix elements that grow exponentially with fragment separation R (note, this is not the same as growing with $|\mathbf{r} - \mathbf{r}'|$).

Of course, the exact ground-state functional is not known, so the second case considered here is the situation for local and semilocal functionals, LDA/GGA. With local approximations, the ϵ_H in Equation 14 is a significant underestimate of the ionization energy: Because the LDA/GGA potentials depend only (semi)locally on the density, and the density falls exponentially with the distance from the atom, the LDA/GGA potentials go to zero exponentially instead of having the slower $-1/r$ tail away from a finite system. Although this does not affect the lower-energy orbitals occupied in the ground state so severely, the valence levels that probe these regions further from the atom get pushed upward, and hence the LDA/GGA HOMO (and LUMO) orbital energies are too small. Tozer (79) showed that the error for charge-transfer excitations when using these functionals tends to the average of the derivative discontinuities of the donor and acceptor: $\omega_q = I^D - A^A - 1/2(\Delta_{XC}^D + \Delta_{XC}^A)$. This is unchanged by the TDDFT correction from f_{XC} due to the local nature of the kernel in LDA/GGA. As a fix, configuration-interaction singles (CIS) was added to simply shift the LDA/GGA values, as described by Dreuw et al. (95); CIS alone gives the $-1/R$ behavior but tends to the Hartree-Fock orbital energy difference, which gives an overestimate. A fix that stays within TDDFT was provided by Gritsenko & Baerends (96) applying a kernel that switches on an asymptotic correction to ALDA when the f_{XC} matrix element becomes too small.

The third case is, in a sense, a functional approximation at the opposite extreme of DFT: exact exchange (EXX). In contrast to LDA, this has a nonlocal dependence on the density (not to be confused with still providing a local multiplicative potential). EXX has a fundamental importance complementary to that of LDA in that it results from first-order (Görling-Levy) perturbation theory in the electron interaction with respect to the KS system (97, 98). Because the EXX potential does have the correct $-1/r$ behavior far from a finite system, the KS HOMO orbital energy approximates the true ionization energy much better than LDA does. Furthermore, through

orbital dependence, the TDEXX kernel contains the required diverging property as a function of R (36, 99–101), yielding both the exchange component to the derivative discontinuity Δ_X as well as the $-1/R$. Frequency dependence is an important aspect: If the adiabatic EXX kernel, $f_{XC}(\omega = 0)$, is used, the correction vanishes instead as $R \rightarrow 0$ (36). The EXX kernel must be evaluated at the charge-transfer excitation energy in order to yield a finite correction; this is related to the strong frequency dependence of the derivative discontinuity of the xc kernel (36, 102).

Next are global hybrid functionals, popular throughout quantum chemistry. These functionals combine a fraction of Hartree-Fock exchange with a local or semilocal functional; for example, with the ubiquitous B3LYP, the fraction is $a_X = 1/4$. Hybrid functionals fall within the generalized KS formulation (86–88), in which the formal justification arises from including a fraction of the electron–electron interaction W in the minimization of $T + a_X W$ over Slater determinants that yield a fixed density; the pure KS DFT approach, however, minimizes only the kinetic energy T. The generalized KS potential is no longer identical for each orbital and is nonlocal (i.e., nonmultiplicative), as it includes a fraction of the Hartree-Fock potential. As a result, the HOMO orbital experiences a $-a_X/r$ potential asymptotically away from a finite system instead of the exponential falloff of (semi)local functionals, so its energy is not as badly underestimated. Further, the LUMO eigenvalue includes this fraction of the exchange contribution to the derivative discontinuity (87); this reflects the partial affinity nature of the unoccupied levels in a hybrid, because in Hartree-Fock the unoccupied orbitals see an $(N + 1)$–electron system, while in pure KS DFT, they see an N-electron system. This also underlies the difference between EXX performed with an optimized effective potential and Hartree-Fock. Thus, hybrids reduce the underestimation of the orbital energy difference for a charge-transfer excitation. Additionally, the Fock-exchange contributes as $-a_X/R$ at large separations to the f_{XC} correction. That is, the KS orbital energy difference provides a partial derivative discontinuity, while the f_{XC} correction partially provides the asymptotic behavior with R.

The global hybrid nudges us toward the correct excitation energy, but the range-separated hybrid (RSH) takes us further by recovering the full Hartree-Fock exchange at large electron–electron separation (103, 104). The idea is to split the Coulomb interaction into long- and short-range terms, such as

$$\frac{1}{|\mathbf{r}_1 - \mathbf{r}_2|} = \frac{\text{erf}(\gamma |\mathbf{r}_1 - \mathbf{r}_2|)}{|\mathbf{r}_1 - \mathbf{r}_2|} + \frac{1 - \text{erf}(\gamma |\mathbf{r}_1 - \mathbf{r}_2|)}{|\mathbf{r}_1 - \mathbf{r}_2|}, \qquad 15.$$

and use local or semilocal approximation for the second term, which dominates at short distances and dies off at long range, while using Hartree-Fock for the first term, which dominates at long range and dies at short range. The range-separation parameter γ controls the distance at which the long-range part begins to take over: The larger the γ is, the smaller the distance at which the Hartree-Fock kicks in. This approach balances the advantages of the Hartree-Fock and semilocal DFT worlds, capturing dynamical correlation and taking advantage of the error cancellation between exchange and correlation from semilocal DFT at short range, while using Hartree-Fock for the long-range interaction that is dominated by exchange and poorly captured by semilocal DFT. Variations of this essential idea include also using some Hartree-Fock at short range; the CAM-B3LYP combines RSH with B3LYP, including a third parameter in the range separation such that there is a nonuniform fraction of Hartree-Fock exchange at all separations (105–107). For the problem of charge transfer, RSH yields the exact $-1/R$ dependence at large R and gives an approximate discontinuity correction to the LUMO orbital energy, moving it toward the physical electron affinity of the donor (108). A challenge is in the empiricism: finding parameters that yield a balanced description of charge transfer as well as local valence and Rydberg excitations in addition to ground-state properties. The results can be very sensitive to these parameters (82).

Global hybrid: fraction of Hartree-Fock exchange + a (semi)local functional

RSH: range-separated hybrid; includes full Hartree-Fock exchange at large range

Also, different range-separated forms have been explored, including some with density-dependent parameters (109, 110); some forms tend to yield a more uniform performance than others (111, 112).

To avoid empiricism completely, Baer, Kronik, and coworkers (110, 113, 114) and Körzdörfer & Brédas (115) developed optimally tuned RSH, in which the range-separation parameter is chosen to minimize the difference between the ionization potential of the donor and the donor's HOMO eigenvalue as well as the difference between the electron affinity of the acceptor and the acceptor's LUMO eigenvalue, all determined consistently with the same functional. The method is arguably the most predictive of the different approximations for charge-transfer excitations between closed-shell fragments and also captures local outer-valence excitations well (116). Still, there are several issues with RSH that should be kept in mind. The potential energy surfaces for triplets and singlets can show erratic zigzagging behavior due to the tuning; this does not happen when the range-separation parameter is fixed (117). RSH violates size consistency (115, 117) and, furthermore, the values for the RSH parameter found by optimal tuning to the ionization potential and electron affinity tend not to give good ground-state binding (118).

Finally, other approximations that have shown some degree of success in capturing charge-transfer excitations include the self-interaction-corrected LDA (119, 120) applied within a generalized time-dependent-optimized effective potential framework (121). As pointed out in Reference 122, the appearance of a finite derivative discontinuity in a functional is related to its correction of self-interaction. The heavy computational cost of this approach has limited its application. However, a less expensive approach that was recently shown to have promise with charge-transfer excitations is the TASK meta-GGA (123): Nonlocality arises through its orbital dependence such that it yields response properties similar to exact exchange but without the numerical cost and gives some improvement of medium-range charge-transfer excitation energies (124). Double-hybrid functionals that combine a second-order correlation part to GGA for correlation on top of a usual hybrid functional have been explored (125), and so have highly parameterized functionals such as M06-HF meta-GGA and MN15 that use many parameters fit to data sets (126, 127).

4.2. Charge-Transfer Excitations Between Open-Shell Fragments

The analysis of the charge-transfer problem for TDDFT is quite distinct from the previous case in which the neutral molecule is composed of open-shell fragments, such as in a heteroatomic diatomic molecule. There is a fundamental difference in the nature of the KS HOMO and LUMO compared to the closed-shell fragments case that makes the previous analysis not applicable. With open-shell fragments, the exact KS singlet ground state has a doubly occupied HOMO orbital that is delocalized over both fragments, quite in contrast to the localized HOMO of the closed-shell case. The LUMO is also delocalized, and its orbital energy becomes degenerate with the HOMO in the limit of infinite separation. The static correlation in the KS system means that at large separations, the ground-state KS Slater determinant has a fundamentally different structure from the interacting wave function, which has a Heitler-London form in contrast to the closed-shell fragment case.

While the ground-state situation is pathological for approximate TDDFT, it is an important one for systems away from equilibrium, such as in bond breaking. The excitations are essential to get right for accurate dynamics in, for example, photodissociation processes.

The exact ground-state KS potential of the widely separated molecule is locally similar to that of the atoms in the vicinity of each atom but has a step in between of a size approaching the difference in the ionization potentials of the two atoms (see **Figure 1c** and the sidebar titled Step in the Ground-State Kohn-Sham Potential) (92, 93, 128–130). This makes the atomic HOMOs line

STEP IN THE GROUND-STATE KOHN-SHAM POTENTIAL

An explicit demonstration of the step in the ground-state Kohn-Sham (KS) potential for the case of open-shell fragments follows from simply considering the KS equation for the external potential

$$v_{\text{ext}}(\mathbf{r}) = v_a(\mathbf{r}) + v_b(\mathbf{r}),$$

where $v_a(\mathbf{r})(v_b(\mathbf{r}))$ represents the electron–nuclear potential for atom $a(b)$ localized around $r = -R/2(R/2)\hat{n}$, where $\hat{n}$ is the interatomic axis with origin at the midpoint between the atoms. The potentials $v_a(\mathbf{r})$ and $v_b(\mathbf{r})$ each support an odd number of electrons in their atomic ground states, and, for large separations R, the highest occupied molecular orbital (HOMO) of the diatomic molecule has the form

$$\phi^{\text{H}}(\mathbf{r}) = \sqrt{\left(|\phi_a^{\text{H}}(\mathbf{r})|^2 + |\phi_b^{\text{H}}(\mathbf{r})|^2\right)/2},$$

with $\phi_a^{\text{H}}(\phi_b^{\text{H}})$ the atomic HOMO of atom $a(b)$ localized at $-R/2(R/2)\hat{n}$.

Now consider the ground-state KS equation in the vicinity of atom a when the intermolecular separation R is large: Here $v_{\text{ext}}(\mathbf{r}) \approx v_a(\mathbf{r}) - Z_b/R$, $v_{\text{H}}[n](\mathbf{r}) \approx v_{\text{H}}[n_a](\mathbf{r}) + N_b/R$, where Z_b and N_b are atom b's nuclear charge and electron number, respectively. Then, for neutral atoms, the KS equation for the molecular HOMO near atom a is

$$\left[-\nabla^2/2 + v_a(\mathbf{r}) + v_{\text{H}}[n_a](\mathbf{r}) + v_{\text{XC}}[n](\mathbf{r})\right]\phi^{\text{H}}(\mathbf{r}) = \epsilon^{\text{H}}\phi^{\text{H}}(\mathbf{r}), \quad \phi^{\text{H}}(\mathbf{r}) \approx \phi_a^{\text{H}}(\mathbf{r})/\sqrt{2}.$$

But we also know that the atomic HOMO satisfies the atomic KS equation

$$\left[-\nabla^2/2 + v_a(\mathbf{r}) + v_{\text{H}}[n_a](\mathbf{r}) + v_{\text{XC}}[n_a](\mathbf{r})\right]\phi_a^{\text{H}}(\mathbf{r}) = \epsilon_a^{\text{H}}\phi_a^{\text{H}}(\mathbf{r}),$$

which means that the difference in the exchange correlation (xc) potential of the molecule compared with that of the atom near atom a is

$$\Delta v_{\text{XC}}[n](\mathbf{r} \approx -R/2) \equiv v_{\text{XC}}[n](\mathbf{r}) - v_{\text{XC}}[n_a](\mathbf{r}) = \epsilon^{\text{H}} - \epsilon_a^{\text{H}}.$$

The same argument applied near atom b leads to $\Delta v_{\text{XC}}[n](\mathbf{r} \approx R/2) \equiv v_{\text{XC}}[n](\mathbf{r}) - v_{\text{XC}}[n_b](\mathbf{r}) = \epsilon^{\text{H}} - \epsilon_b^{\text{H}}$. Thus, across the molecule, there is a step in the difference of the molecular xc potential compared to those of the atomic xc potentials:

$$\Delta v_{\text{XC}}[n](\mathbf{r} \approx R/2) - \Delta v_{\text{XC}}[n](\mathbf{r} \approx -R/2) = \epsilon_a^{\text{H}} - \epsilon_b^{\text{H}} = I_b - I_a.$$

An illustration of the ground-state KS potential and orbitals is shown in **Figure 1c**.

up in order for the molecular HOMO to correctly straddle both atoms and capture the correct ground-state density. However, the interatomic step is not captured by approximate functionals: The semilocal molecular HOMO is delocalized over both atoms but does not reduce to the combination of the atomic HOMOs, and the molecule unphysically dissociates to fractionally charged species. Hybrid functionals, including RSH, also do not dissociate correctly into the neutral atomic species. This is true for general N and can be seen simply by considering a model heteroatomic two-electron system in which there is one electron on each atom: For two electrons, the Hartree-Fock exchange potential is $-v_{\text{H}}/2$, so that in the vicinity of each atom in the widely separated limit, $v_{\text{S}} = v_{\text{ext}} + v_{\text{H}}/2$, while it should be v_{ext}. The local atomic densities are wrong. A functional that was inspired by density-matrix functional theory with explicit dependence on both occupied and virtual orbitals has been shown to capture the step structure (131, 132), but whether this can be turned into a practical approach remains to be seen. Static correlation is well-known to be a difficult regime for density functional approximations in the ground state, and its implications for excitation energies and response are very challenging; some recent progress based on the strictly correlated electron approach for dissociation can be found in References 133–135.

All KS excitations of such a system are near degenerate, with a double excitation where both electrons are excited out of the HOMO; an additional excitation from the HOMO to the LUMO adds very little cost to a single excitation from the HOMO to any unoccupied orbital. Both HOMO and LUMO are delocalized over both atoms and have substantial overlap, with an orbital energy difference that vanishes exponentially with the separation R (54, 55, 78); however, these are the orbitals involved in the lowest charge-transfer excitations of the molecule. As the bare KS excitation energy ω_q between the HOMO and LUMO vanishes exponentially with separation R, the TDDFT corrections in the matrix elements involving f_{XC} are responsible for the entire charge-transfer energy of Equation 13. Furthermore, if one were to simplify the analysis through considering only the HOMO-LUMO excitation subspace, one would observe that Equation 9 is not valid, as the ω_q is smaller than the correction. Within the SMA (Equation 8), the exact f_{XC} matrix element has a very strong frequency dependence and diverges exponentially with the fragment separation R (54, 55, 78). The exact-exchange kernel (36, 101) discussed briefly in Section 4.1 displays a frequency-dependent divergence with respect to R, but in the present case, the divergence occurs in the correlation kernel. In fact, throughout all frequencies, the xc kernel in the present case is rife with strong-frequency dependence. This can be understood as being due to mixing with the near-degenerate double excitations throughout the spectrum. Physically, this mixing is essential to avoid yielding excited states that have half an electron excess or deficit on one atom (see also **Figure 1c**).

5. OUTLOOK

Although at equilibrium geometries, double excitations may be relevant in relatively few situations, they are absolutely crucial in coupled electron–ion dynamics following an excitation or driven by a laser. Levine and coworkers (136) pointed out that, even if problematic excitations are not present at the equilibrium geometry, photoinduced dynamics traverses large ranges of nuclear configurations, and the likelihood of curve-crossing means that challenging excitations such as double and charge-transfer excitations and conical intersections are likely to be encountered. For example, in ethylene, a $\pi \rightarrow \pi^*$ excitation is followed by twisting and pyramidalization. The global minimum on S_1 is of doubly excited character and at a geometry that is both twisted and pyramidalized, but the absence of double excitations in adiabatic TDDFT yields an S_1 minimum that is purely twisted (136). This would clearly alter the predictions of the coupled electron–nuclear dynamics.

Likewise, long-range charge-transfer excitations of a molecule are highly relevant for the dynamics of a molecule following a photoexcitation out of the ground state of its equilibrium geometry or driven by a laser field. In these situations, the propensity for dissociating is increased for either the closed-shell or open-shell fragment case. The coupled electronic and nuclear motion straddles several Born-Oppenheimer potential energy surfaces, and for TDDFT to be used reliably in mixed quantum-classical Ehrenfest or surface-hopping calculations, the surfaces obtained from linear-response TDDFT must be globally accurate to get accurate dynamics. Indeed, the lack of computationally efficient and reliably accurate electronic structure methods is arguably the main hindrance to nonadiabatic dynamics calculations, more so than the choice of method used for the electron–nuclear correlation: All the methods used to couple the electronic and nuclear motion would greatly benefit from improved functional approximations in TDDFT, especially for double excitations, charge-transfer excitations, and conical intersections. Whether developments uncovering and modeling the memory dependence of exact functionals in the real-time domain can lead to new approximations for linear response remains to be seen (137). Out of wavefunction methods that may be more reliable for these excitations, one would wish to avoid issues such as inadequacy of chosen active spaces as the molecule explores geometries in which the electronic structure has significantly changed character or is not well understood, e.g., in CASSCF and

related methods, which, at the same time, are limited to much smaller molecules than possible with TDDFT, and even more so with coupled-cluster methods. Even if possible with expanding computational architectures, running expensive calculations that use a lot of computational power should be carefully justified in the current climate crisis. The problem also urges forward the further exploration of other reduced-variable theories, including the ensemble DFT [that was discussed in application to double excitations in Section 3.2 and that has also been applied to charge-transfer excitations (138, 139)], Green's function and Bethe-Salpeter methods (140–143), and one-body density-matrix functional theory (144–146). Future years hope to see further significant progress continuing from that made in recent decades, with ever-improving numerical implementations as well as new and exciting applications yet to be imagined.

SUMMARY POINTS

1. Time-dependent density functional theory (TDDFT) provides an elegant and rigorous way to obtain electronic excitations and response for many-electron systems that has achieved an unrivaled balance between accuracy and efficiency. The acrobatics of the functionals involved that allow noninteracting electrons to reproduce the exact density of an interacting system remain an intriguing, important, and fun research area.

2. There are certain excitations for which the standard functionals that are semilocal in space and local in time in their dependence on the density do not perform well, such as double excitations and charge-transfer excitations.

3. There has been significant process in developing functionals with improved accuracy and reliability over recent years that address these challenging excitations in a nonempirical way. For double excitations, a strong frequency dependence is required in the exchange correlation (xc) kernel, while for many, but not all, classes of charge-transfer excitations, spatial nonlocality is more important.

FUTURE ISSUES

1. We can look forward to further progress in turning the recent developments into black-box methods, from the algorithmic and computational point of view (e.g., practical treatment of frequency-dependent functionals) and in developments to ease the computational efficiency to benefit photochemical dynamics applications with the more accurate functionals.

2. A related point is that the treatment of conical intersections with the ground state remains a challenge.

3. Understanding the performance of the full response properties beyond merely the value of the excitation energies (e.g., oscillator strengths) from the newer functionals will lead to more food for thought.

4. The exactness of the underlying theory offers hope that further development of first-principles functionals from different starting points may lead to improved future robust, reliable, and predictive functional approximations.

DISCLOSURE STATEMENT

ACKNOWLEDGMENTS

LITERATURE CITED

1. Runge E, Gross EKU. 1984. Density-functional theory for time-dependent systems. *Phys. Rev. Lett.* 52(12):997–1000
2. Casida M. 1995. Time-dependent density functional response theory for molecules. In *Recent Advances in Density Functional Methods, Part I*, ed. DP Chong, pp. 155–92. Singapore: World Sci.
3. Petersilka M, Gossmann UJ, Gross EKU. 1996. Excitation energies from time-dependent density-functional theory. *Phys. Rev. Lett.* 76(8):1212–15
4. Loos PF, Boggio-Pasqua M, Scemama A, Caffarel M, Jacquemin D. 2019. Reference energies for double excitations. *J. Chem. Theory Comput.* 15(3):1939–56
5. Véril M, Scemama A, Caffarel M, Lipparini F, Boggio-Pasqua M, et al. 2021. QUESTDB: a database of highly accurate excitation energies for the electronic structure community. *WIREs Comput. Mol. Sci.* 11(5):e1517

6. Ullrich CA. 2011. *Time-Dependent Density-Functional Theory: Concepts and Applications*. Oxford, UK: Oxford Univ. Press

7. Marques MAL, Maitra NT, Nogueira FMS, Gross EKU, Rubio A, eds. 2012. *Fundamentals of Time-Dependent Density Functional Theory*. Lect. Notes Phys. Vol. 837. Berlin/Heidelberg: Springer-Verlag

8. Maitra NT. 2016. Fundamental aspects of time-dependent density functional theory. *J. Chem. Phys.* 144(22):220901

9. Casida M, Huix-Rotllant M. 2012. Progress in time-dependent density-functional theory. *Annu. Rev. Phys. Chem.* 63:287–323

10. Hohenberg P, Kohn W. 1964. Inhomogeneous electron gas. *Phys. Rev.* 136(3B):B864–71
11. Casida ME. 1996. Time-dependent density functional response theory of molecular systems: theory, computational methods, and functionals. In *Recent Developments and Applications of Modern Density Functional Theory*, ed. JM Seminario, pp. 391–440. Theor. Comput. Chem. Vol. 4. Amsterdam: Elsevier
12. Gross EK, Maitra NT. 2012. Introduction to TDDFT. In *Fundamentals of Time-Dependent Density Functional Theory*, ed. MAL Marques, NT Maitra, FMS Nogueira, EKU Gross, A Rubio, pp. 53–99. Lect. Notes Phys. Vol. 837. Berlin/Heidelberg: Springer-Verlag
13. Grabo T, Petersilka M, Gross E. 2000. Molecular excitation energies from time-dependent density functional theory. *J. Mol. Struct.* 501–502:353–67
14. Appel H, Gross EKU, Burke K. 2003. Excitations in time-dependent density-functional theory. *Phys. Rev. Lett.* 90(4):043005
15. Burke K. 2012. Perspective on density functional theory. *J. Chem. Phys.* 136(15):150901
16. Becke AD. 2014. Fifty years of density-functional theory in chemical physics. *J. Chem. Phys.* 140(18):18A301
17. Yu HS, Li SL, Truhlar DG. 2016. Kohn-Sham density functional theory descending a staircase. *J. Chem. Phys.* 145(13):130901
18. Goerigk L, Mehta N. 2019. A trip to the density functional theory zoo: warnings and recommendations for the user. *Aust. J. Chem.* 72:563–73

6. A pedagogical book on the theory, formalism, and performance of TDDFT for finite and extended systems.

8. An overview of theory and challenges in both the linear response and nonperturbative regimes in TDDFT.

9. A review on TDDFT for excitations.

19. Sternheimer RM. 1954. Electronic polarizabilities of ions from the Hartree-Fock wave functions. *Phys. Rev.* 96(4):951–68

20. Andrade X, Botti S, Marques MAL, Rubio A. 2007. Time-dependent density functional theory scheme for efficient calculations of dynamic (hyper)polarizabilities. *J. Chem. Phys.* 126(18):184106

21. Yabana K, Nakatsukasa T, Iwata JI, Bertsch G. 2006. Real-time, real-space implementation of the linear response time-dependent density-functional theory. *Phys. Status Solidi B* 243(5):1121–38

22. Elliott P, Goldson S, Canahui C, Maitra NT. 2011. Perspectives on double-excitations in TDDFT. *Chem. Phys.* 391(1):110–19

23. Zhang F, Burke K. 2004. Adiabatic connection for near degenerate excited states. *Phys. Rev. A* 69(5):052510

24. Brandenburg JG, Burke K, Fromager E, Gatti M, Giarrusso S, et al. 2020. New approaches to study excited states in density functional theory: general discussion. *Faraday Discuss.* 224:483–508

25. Shu Y, Truhlar DG. 2017. Doubly excited character or static correlation of the reference state in the controversial 2^1A_g state of *trans*-butadiene? *J. Am. Chem. Soc.* 139(39):13770–78

26. Barca GMJ, Gilbert ATB, Gill PMW. 2018. Excitation number: characterizing multiply excited states. *J. Chem. Theory Comput.* 14(1):9–13

27. Jamorski C, Casida ME, Salahub DR. 1996. Dynamic polarizabilities and excitation spectra from a molecular implementation of time-dependent density-functional response theory: N_2 as a case study. *J. Chem. Phys.* 104(13):5134–47

28. Tozer DJ, Handy NC. 2000. On the determination of excitation energies using density functional theory. *Phys. Chem. Chem. Phys.* 2(10):2117–21

29. Maitra NT, Zhang F, Cave RJ, Burke K. 2004. Double excitations within time-dependent density functional theory linear response. *J. Chem. Phys.* 120(13):5932–37

30. Authier J, Loos PF. 2020. Dynamical kernels for optical excitations. *J. Chem. Phys.* 153(18):184105

31. Thiele M, Kümmel S. 2009. Photoabsorption spectra from adiabatically exact time-dependent density-functional theory in real time. *Phys. Chem. Chem. Phys.* 11(22):4631–39

32. Thiele M, Kümmel S. 2014. Frequency dependence of the exact exchange-correlation kernel of time-dependent density-functional theory. *Phys. Rev. Lett.* 112(8):083001

33. Entwistle MT, Godby RW. 2019. Exact exchange-correlation kernels for optical spectra of model systems. *Phys. Rev. B* 99(16):161102

34. Woods ND, Entwistle MT, Godby RW. 2021. Insights from exact exchange-correlation kernels. *Phys. Rev. B* 103(12):125155

35. Hellgren M, von Barth U. 2008. Linear density response function within the time-dependent exact-exchange approximation. *Phys. Rev. B* 78(11):115107

36. Hellgren M, Gross EKU. 2012. Discontinuities of the exchange-correlation kernel and charge-transfer excitations in time-dependent density-functional theory. *Phys. Rev. A* 85(2):022514

37. Ruggenthaler M, Nielsen SE, Van Leeuwen R. 2013. Analytic density functionals with initial-state dependence and memory. *Phys. Rev. A* 88(2):022512

38. Fuks JI, Maitra NT. 2014. Challenging adiabatic time-dependent density functional theory with a Hubbard dimer: the case of time-resolved long-range charge transfer. *Phys. Chem. Chem. Phys.* 16(28):14504–13

39. Aryasetiawan F, Gunnarsson O. 2002. Exchange-correlation kernel in time-dependent density functional theory. *Phys. Rev. B* 66(16):165119

40. Turkowski V, Rahman TS. 2013. Nonadiabatic time-dependent spin-density functional theory for strongly correlated systems. *J. Phys. Condens. Matter* 26(2):022201

41. Carrascal DJ, Ferrer J, Maitra N, Burke K. 2018. Linear response time-dependent density functional theory of the Hubbard dimer. *Eur. Phys. J. B* 91:142

42. Cave RJ, Zhang F, Maitra NT, Burke K. 2004. A dressed TDDFT treatment of the 2^1A_g states of butadiene and hexatriene. *Chem. Phys. Lett.* 389(1–3):39–42

43. Mazur G, Wlodarczyk R. 2009. Application of the dressed time-dependent density functional theory for the excited states of linear polyenes. *J. Comput. Chem.* 30(5):811–17

44. Mazur G, Makowski M, Wldarczyk R, Aoki Y. 2011. Dressed TDDFT study of low-lying electronic excited states in selected linear polyenes and diphenylopolyenes. *Int. J. Quant. Chem.* 111(4):819–25

45. Gritsenko OV, Baerends EJ. 2009. Double excitation effect in non-adiabatic time-dependent density functional theory with an analytic construction of the exchange-correlation kernel in the common energy denominator approximation. *Phys. Chem. Chem. Phys.* 11(22):4640–46

46. Casida ME. 2005. Propagator corrections to adiabatic time-dependent density-functional theory linear response theory. *J. Chem. Phys.* 122(5):054111

47. Romaniello P, Sangalli D, Berger JA, Sottile F, Molinari LG, et al. 2009. Double excitations in finite systems. *J. Chem. Phys.* 130(4):044108

48. Bruneval F, Sottile F, Olevano V, Del Sole R, Reining L. 2005. Many-body perturbation theory using the density-functional concept: beyond the *GW* approximation. *Phys. Rev. Lett.* 94(18):186402

49. Gatti M, Olevano V, Reining L, Tokatly IV. 2007. Transforming nonlocality into a frequency dependence: a shortcut to spectroscopy. *Phys. Rev. Lett.* 99(5):057401

50. Sangalli D, Romaniello P, Onida G, Marini A. 2011. Double excitations in correlated systems: a many-body approach. *J. Chem. Phys.* 134(3):034115

51. Casida ME, Huix-Rotllant M. 2016. Many-body perturbation theory (MBPT) and time-dependent density-functional theory (TD-DFT): MBPT insights about what is missing in, and corrections to, the TD-DFT adiabatic approximation. In *Density-Functional Methods for Excited States*, ed. N Ferré, M Filatov, M Huix-Rotllant, pp. 1–60. Top. Curr. Chem. Vol. 368. Cham, Switz.: Springer Int. Publ.

52. Huix-Rotllant M, Ipatov A, Rubio A, Casida ME. 2011. Assessment of dressed time-dependent density-functional theory for the low-lying valence states of 28 organic chromophores. *Chem. Phys.* 391(1):120–29

53. Köster AM, Calaminici P, Casida ME, Flores-Moreno R, Geudtner G, et al. 2006. demon2k@grenoble. The International deMon Developers Community (Cinvestav-IPN, Mexico)

54. Maitra NT, Tempel DG. 2006. Long-range excitations in time-dependent density functional theory. *J. Chem. Phys.* 125(18):184111

55. Maitra NT. 2005. Undoing static correlation: long-range charge transfer in time-dependent density-functional theory. *J. Chem. Phys.* 122(23):234104

56. Tapavicza E, Tavernelli I, Rothlisberger U, Filippi C, Casida ME. 2008. Mixed time-dependent density-functional theory/classical trajectory surface hopping study of oxirane photochemistry. *J. Chem. Phys.* 129(12):124108

57. Gritsenko OV, van Gisbergen SJA, Görling A, Baerends EJ. 2000. Excitation energies of dissociating H_2: a problematic case for the adiabatic approximation of time-dependent density functional theory. *J. Chem. Phys.* 113(19):8478–89

58. Sarkar R, Boggio-Pasqua M, Loos PF, Jacquemin D. 2021. Benchmarking TD-DFT and wave function methods for oscillator strengths and excited-state dipole moments. *J. Chem. Theory Comput.* 17(2):1117–32

59. Tretiak S, Chernyak V. 2003. Resonant nonlinear polarizabilities in the time-dependent density functional theory. *J. Chem. Phys.* 119(17):8809–23

60. Shao Y, Head-Gordon M, Krylov AI. 2003. The spin–flip approach within time-dependent density functional theory: theory and applications to diradicals. *J. Chem. Phys.* 118(11):4807–18

61. Rinkevicius Z, Vahtras O, Ågren H. 2010. Spin-flip time dependent density functional theory applied to excited states with single, double, or mixed electron excitation character. *J. Chem. Phys.* 133(11):114104

62. Wang F, Ziegler T. 2005. The performance of time-dependent density functional theory based on a noncollinear exchange-correlation potential in the calculations of excitation energies. *J. Chem. Phys.* 122(7):074109

63. Yang Y, van Aggelen H, Yang W. 2013. Double, Rydberg and charge transfer excitations from pairing matrix fluctuation and particle-particle random phase approximation. *J. Chem. Phys.* 139(22):224105

64. Yang Y, Peng D, Lu J, Yang W. 2014. Excitation energies from particle-particle random phase approximation: Davidson algorithm and benchmark studies. *J. Chem. Phys.* 141(12):124104

65. Hait D, Head-Gordon M. 2021. Orbital optimized density functional theory for electronic excited states. *J. Phys. Chem. Lett.* 12(19):4517–29

66. Seidu I, Krykunov M, Ziegler T. 2014. The formulation of a constricted variational density functional theory for double excitations. *Mol. Phys.* 112(5–6):661–68

67. Ramos P, Pavanello M. 2018. Low-lying excited states by constrained DFT. *J. Chem. Phys.* 148(14):144103

68. Gross EKU, Oliveira LN, Kohn W. 1988. Density-functional theory for ensembles of fractionally occupied states. I. Basic formalism. *Phys. Rev. A* 37(8):2809–20

69. Gross EKU, Oliveira LN, Kohn W. 1988. Rayleigh-Ritz variational principle for ensembles of fractionally occupied states. *Phys. Rev. A* 37(8):2805–8

70. Oliveira LN, Gross EKU, Kohn W. 1988. Density-functional theory for ensembles of fractionally occupied states. II. Application to the He atom. *Phys. Rev. A* 37(8):2821–33

71. Gidopoulos NI, Papaconstantinou PG, Gross EKU. 2002. Spurious interactions, and their correction, in the ensemble-Kohn-Sham scheme for excited states. *Phys. Rev. Lett.* 88(3):033003

72. Tasnádi F, Nagy Á. 2003. An approximation to the ensemble Kohn–Sham exchange potential for excited states of atoms. *J. Chem. Phys.* 119(8):4141–47

73. Sagredo F, Burke K. 2018. Accurate double excitations from ensemble density functional calculations. *J. Chem. Phys.* 149(13):134103

74. Loos PF, Fromager E. 2020. A weight-dependent local correlation density-functional approximation for ensembles. *J. Chem. Phys.* 152(21):214101

75. Marut C, Senjean B, Fromager E, Loos PF. 2020. Weight dependence of local exchange–correlation functionals in ensemble density-functional theory: double excitations in two-electron systems. *Faraday Discuss.* 224(0):402–23

76. Pribram-Jones A, Yang Z, Trail JR, Burke K, Needs RJ, Ullrich CA. 2014. Excitations and benchmark ensemble density functional theory for two electrons. *J. Chem. Phys.* 140(18):18A541

77. Kaduk B, Kowalczyk T, Van Voorhis T. 2012. Constrained density functional theory. *Chem. Rev.* 112(1):321–70

78. Maitra NT. 2017. Charge transfer in time-dependent density functional theory. *J. Phys. Condens. Matter* 29(42):423001

79. Tozer DJ. 2003. Relationship between long-range charge-transfer excitation energy error and integer discontinuity in Kohn-Sham theory. *J. Chem. Phys.* 119(24):12697–99

80. Dreuw A, Head-Gordon M. 2004. Failure of time-dependent density functional theory for long-range charge-transfer excited states: the zincbacteriochlorin-bacteriochlorin and bacteriochlorophyll-spheroidene complexes. *J. Am. Chem. Soc.* 126(12):4007–16

81. Rappoport D, Furche F. 2004. Photoinduced intramolecular charge transfer in 4-(dimethyl)aminobenzonitrile – a theoretical perspective. *J. Am. Chem. Soc.* 126(4):1277–84

82. Kümmel S. 2017. Charge-transfer excitations: a challenge for time-dependent density functional theory that has been met. *Adv. Energy Mater.* 7(16):1700440

83. Peach MJG, Benfield P, Helgaker T, Tozer DJ. 2008. Excitation energies in density functional theory: an evaluation and a diagnostic test. *J. Chem. Phys.* 128(4):044118

84. Guido CA, Cortona P, Mennucci B, Adamo C. 2013. On the metric of charge transfer molecular excitations: a simple chemical descriptor. *J. Chem. Theory Comput.* 9(7):3118–26

85. Li Y, Ullrich CA. 2016. The particle-hole map: formal derivation and numerical implementation. *J. Chem. Phys.* 145(16):164107

86. Garrick R, Natan A, Gould T, Kronik L. 2020. Exact generalized Kohn-Sham theory for hybrid functionals. *Phys. Rev. X* 10(2):021040

87. Seidl A, Görling A, Vogl P, Majewski JA, Levy M. 1996. Generalized Kohn-Sham schemes and the band-gap problem. *Phys. Rev. B* 53(7):3764–74

88. Görling A, Levy M. 1997. Hybrid schemes combining the Hartree–Fock method and density-functional theory: underlying formalism and properties of correlation functionals. *J. Chem. Phys.* 106(7):2675–80

89. Grabo T, Kreibich T, Kurth S, Gross E. 2000. Orbital functionals in density functional theory: the optimized effective potential method. In *Strong Coulomb Correlations in Electronic Structure Calculations: Beyond the Local Density Approximation*, ed. VI Anisimov, pp. 203–96. Adv. Condens. Matter Sci. Vol. 1. Amsterdam: Gordon and Breach

90. Perdew JP, Levy M. 1983. Physical content of the exact Kohn-Sham orbital energies: band gaps and derivative discontinuities. *Phys. Rev. Lett.* 51(20):1884–87

78. A review of charge-transfer excitations as well as full charge-transfer dynamics in TDDFT.

82. An overview of the use of optimally tuned RSH for charge-transfer excitations.

91. Sham LJ, Schlüter M. 1983. Density-functional theory of the energy gap. *Phys. Rev. Lett.* 51(20):1888–91

92. Perdew JP. 1985. What do the Kohn-Sham orbital energies mean? How do atoms dissociate? In *Density-Functional Methods in Physics*, ed. RM Dreizler, J da Providência, pp. 265–308. New York: Plenum

93. Almbladh CO, von Barth U. 1985. Exact results for the charge and spin densities, exchange-correlation potentials, and density-functional eigenvalues. *Phys. Rev. B* 31(6):3231–44

94. Perdew JP, Parr RG, Levy M, Balduz JL. 1982. Density-functional theory for fractional particle number: derivative discontinuities of the energy. *Phys. Rev. Lett.* 49(23):1691–94

95. Dreuw A, Weisman JL, Head-Gordon M. 2003. Long-range charge-transfer excited states in time-dependent density functional theory require non-local exchange. *J. Chem. Phys.* 119(6):2943–46

96. Gritsenko O, Baerends EJ. 2004. Asymptotic correction of the exchange–correlation kernel of time-dependent density functional theory for long-range charge-transfer excitations. *J. Chem. Phys.* 121(2):655–60

97. Görling A, Levy M. 1993. Correlation-energy functional and its high-density limit obtained from a coupling-constant perturbation expansion. *Phys. Rev. B* 47(20):13105–13

98. Gonze X, Scheffler M. 1999. Exchange and correlation kernels at the resonance frequency: implications for excitation energies in density-functional theory. *Phys. Rev. Lett.* 82(22):4416–19

99. Heßelmann A, Ipatov A, Görling A. 2009. Charge-transfer excitation energies with a time-dependent density-functional method suitable for orbital-dependent exchange-correlation kernels. *Phys. Rev. A* 80(1):012507

100. Gimon T, Ipatov A, Heßelmann A, Görling A. 2009. Qualitatively correct charge-transfer excitation energies in HeH$^+$ by time-dependent density-functional theory due to exact exchange Kohn-Sham eigenvalue differences. *J. Chem. Theory Comput.* 5(4):781–85

101. Hellgren M, Gross EKU. 2013. Discontinuous functional for linear-response time-dependent density-functional theory: the exact-exchange kernel and approximate forms. *Phys. Rev. A* 88(5):052507

102. Mundt M, Kümmel S. 2005. Derivative discontinuities in time-dependent density-functional theory. *Phys. Rev. Lett.* 95(20):203004

103. Leininger T, Stoll H, Werner HJ, Savin A. 1997. Combining long-range configuration interaction with short-range density functionals. *Chem. Phys. Lett.* 275(3–4):151–60

104. Stoll H, Savin A. 1985. Density functionals for correlation energies of atoms and molecules. In *Density Functional Methods in Physics*, ed. R Dreizler, J da Providência, pp. 177–208. New York: Plenum

105. Iikura H, Tsuneda T, Yanai T, Hirao K. 2001. A long-range correction scheme for generalized-gradient-approximation exchange functionals. *J. Chem. Phys.* 115(8):3540–44

106. Yanai T, Tew DP, Handy NC. 2004. A new hybrid exchange–correlation functional using the Coulomb-attenuating method (CAM-B3LYP). *Chem. Phys. Lett.* 393(1–3):51–57

107. Henderson TM, Janesko BG, Scuseria GE. 2008. Range separation and local hybridization in density functional theory. *J. Phys. Chem. A* 112(49):12530–42

108. Tawada Y, Tsuneda T, Yanagisawa S, Yanai T, Hirao K. 2004. A long-range-corrected time-dependent density functional theory. *J. Chem. Phys.* 120(18):8425–33

109. Baer R, Neuhauser D. 2005. Density functional theory with correct long-range asymptotic behavior. *Phys. Rev. Lett.* 94(4):043002

110. **Baer R, Livshits E, Salzner U. 2010. Tuned range-separated hybrids in density functional theory. *Annu. Rev. Phys. Chem.* 61:85–109**

111. Rohrdanz MA, Martins KM, Herbert JM. 2009. A long-range-corrected density functional that performs well for both ground-state properties and time-dependent density functional theory excitation energies, including charge-transfer excited states. *J. Chem. Phys.* 130(5):054112

112. Henderson TM, Janesko BG, Scuseria GE. 2008. Generalized gradient approximation model exchange holes for range-separated hybrids. *J. Chem. Phys.* 128(19):194105

113. Kronik L, Stein T, Refaely-Abramson S, Baer R. 2012. Excitation gaps of finite-sized systems from optimally tuned range-separated hybrid functionals. *J. Chem. Theory Comput.* 8(5):1515–31

114. Stein T, Kronik L, Baer R. 2009. Reliable prediction of charge transfer excitations in molecular complexes using time-dependent density functional theory. *J. Am. Chem. Soc.* 131(8):2818–20

110. A review on the theory and applications of tuned RSH.

115. Körzdörfer T, Brédas JL. 2014. Organic electronic materials: recent advances in the DFT description of the ground and excited states using tuned range-separated hybrid functionals. *Acc. Chem. Res.* 47(11):3284–91

116. Egger DA, Weissman S, Refaely-Abramson S, Sharifzadeh S, Dauth M, et al. 2014. Outer-valence electron spectra of prototypical aromatic heterocycles from an optimally tuned range-separated hybrid functional. *J. Chem. Theory Comput.* 10(5):1934–52

117. Karolewski A, Kronik L, Kümmel S. 2013. Using optimally tuned range separated hybrid functionals in ground-state calculations: consequences and caveats. *J. Chem. Phys.* 138(20):204115

118. Schmidt T, Kraisler E, Makmal A, Kronik L, Kümmel S. 2014. A self-interaction-free local hybrid functional: accurate binding energies vis-à-vis accurate ionization potentials from Kohn-Sham eigenvalues. *J. Chem. Phys.* 140(18):18A510

119. Hofmann D, Körzdörfer T, Kümmel S. 2012. Kohn-Sham self-interaction correction in real time. *Phys. Rev. Lett.* 108(14):146401

120. Hofmann D, Kümmel S. 2012. Self-interaction correction in a real-time Kohn-Sham scheme: access to difficult excitations in time-dependent density functional theory. *J. Chem. Phys.* 137(6):064117

121. Körzdörfer T, Kümmel S, Mundt M. 2008. Self-interaction correction and the optimized effective potential. *J. Chem. Phys.* 129(1):014110

122. Perdew JP. 1990. Size-consistency, self-interaction correction, and derivative discontinuity in density functional theory. In *Density Functional Theory of Many-Fermion Systems*, ed. P-O Löwdin, pp. 113–34. Adv. Quantum Chem. Vol. 21. Amsterdam: Elsevier

123. Aschebrock T, Kümmel S. 2019. Ultranonlocality and accurate band gaps from a meta-generalized gradient approximation. *Phys. Rev. Res.* 1(3):033082

124. Hofmann F, Kümmel S. 2020. Molecular excitations from meta-generalized gradient approximations in the Kohn–Sham scheme. *J. Chem. Phys.* 153(11):114106

125. Grimme S, Neese F. 2007. Double-hybrid density functional theory for excited electronic states of molecules. *J. Chem. Phys.* 127(15):154116

126. Zhao Y, Truhlar DG. 2006. Density functional for spectroscopy: no long-range self-interaction error, good performance for Rydberg and charge-transfer states, and better performance on average than B3LYP for ground states. *J. Phys. Chem. A* 110(49):13126–30

127. Yu HS, He X, Li SL, Truhlar DG. 2016. Mn15: a Kohn–Sham global-hybrid exchange–correlation density functional with broad accuracy for multi-reference and single-reference systems and noncovalent interactions. *Chem. Sci.* 7(8):5032–51

128. Tempel DG, Martínez TJ, Maitra NT. 2009. Revisiting molecular dissociation in density functional theory: a simple model. *J. Chem. Theory Comput.* 5(4):770–80

129. Gritsenko OV, Baerends EJ. 1996. Effect of molecular dissociation on the exchange-correlation Kohn-Sham potential. *Phys. Rev. A* 54(3):1957–72

130. Helbig N, Tokatly IV, Rubio A. 2009. Exact Kohn–Sham potential of strongly correlated finite systems. *J. Chem. Phys.* 131(22):224105

131. Buijse MA, Baerends EJ. 2002. An approximate exchange-correlation hole density as a functional of the natural orbitals. *Mol. Phys.* 100(4):401–21

132. Gritsenko O, Baerends EJ. 2006. Correct dissociation limit for the exchange-correlation energy and potential. *Int. J. Quantum Chem.* 106(15):3167–77

133. Giarrusso S, Vuckovic S, Gori-Giorgi P. 2018. Response potential in the strong-interaction limit of density functional theory: analysis and comparison with the coupling-constant average. *J. Chem. Theory Comput.* 14(8):4151–67

134. Grossi J, Seidl M, Gori-Giorgi P, Giesbertz KJH. 2019. Functional derivative of the zero-point-energy functional from the strong-interaction limit of density-functional theory. *Phys. Rev. A* 99(5):052504

135. Giarrusso S, Gori-Giorgi P. 2020. Exchange-correlation energy densities and response potentials: connection between two definitions and analytical model for the strong-coupling limit of a stretched bond. *J. Phys. Chem. A* 124(12):2473–82

136. Levine BG, Ko C, Quenneville J, Martínez TJ. 2006. Conical intersections and double excitations in time-dependent density functional theory. *Mol. Phys.* 104(5–7):1039–51

137. Lacombe L, Maitra NT. 2020. Developing new and understanding old approximations in TDDFT. *Faraday Discuss.* 224:382–401

138. Gould T, Kronik L, Pittalis S. 2018. Charge transfer excitations from exact and approximate ensemble Kohn-Sham theory. *J. Chem. Phys.* 148(17):174101

139. Franck O, Fromager E. 2014. Generalised adiabatic connection in ensemble density-functional theory for excited states: example of the H_2 molecule. *Mol. Phys.* 112(12):1684–701

140. Jacquemin D, Duchemin I, Blase X. 2017. Is the Bethe–Salpeter formalism accurate for excitation energies? Comparisons with TD-DFT, CASPT2, and EOM-CCSD. *J. Phys. Chem. Lett.* 8(7):1524–29

141. Liu C, Kloppenburg J, Yao Y, Ren X, Appel H, et al. 2020. All-electron ab initio Bethe-Salpeter equation approach to neutral excitations in molecules with numeric atom-centered orbitals. *J. Chem. Phys.* 152(4):044105

142. Sharifzadeh S. 2018. Many-body perturbation theory for understanding optical excitations in organic molecules and solids. *J. Phys. Condens. Matter* 30(15):153002

143. Loos PF, Blase X. 2020. Dynamical correction to the Bethe–Salpeter equation beyond the plasmon-pole approximation. *J. Chem. Phys.* 153(11):114120

144. Giesbertz KJH, Baerends EJ, Gritsenko OV. 2008. Charge transfer, double and bond-breaking excitations with time-dependent density matrix functional theory. *Phys. Rev. Lett.* 101(3):033004

145. Giesbertz KJH, Pernal K, Gritsenko OV, Baerends EJ. 2009. Excitation energies with time-dependent density matrix functional theory: singlet two-electron systems. *J. Chem. Phys.* 130(11):114104

146. Giesbertz KJH, Gritsenko OV, Baerends EJ. 2010. Response calculations with an independent particle system with an exact one-particle density matrix. *Phys. Rev. Lett.* 105(1):013002